



Insights into the recurrent energetic eruptions on Awu, one of the deadliest volcano on earth

Philipson Bani¹, Kristianto², Syegi Kunrat², Devy Kamil Syahbana²

5

1- Laboratoire Magmas et Volcans, Université Blaise Pascal - CNRS -IRD, OPGC, Aubière, France.

2- Center for Volcanology and Geological Hazard Mitigation (CVGHM), Jl. Diponegoro No. 57, Bandung, Indonesia

Correspondence to: Philipson Bani (philipson.bani@ird.fr)

10 Abstract

The little know Awu volcano is among the deadliest with a cumulative dead toll of 11048. In less than 4 centuries, 18 eruptions were recorded, including two VEI-4 and three VEI-3 with worldwide impacts. The regional geodynamic is controlled by a divergent-double-subduction and an arc-arc collision. In that context, the slab stalls in the mantle, undergoes an increase of temperature and becomes prone to melting, a process that sustained the magmatic supply. Awu also has the particularity to host alternatively and simultaneously a lava dome and a crater lake throughout its activity. The lava dome occurred passively through the crater lake and induced strong water evaporation from the crater. A conduit plug associated with this dome emplacement subsequently channeled the gas emission to the crater wall. However, with the lava dome cooling, the high annual rainfall eventually reconstituted the crater lake and creating a hazardous situation on Awu. Indeed with a new magma injection, rapid pressure buildup may pulverize the conduit plug and the lava dome, allowing lake water injection and subsequent explosive water-magma interaction. The past vigorous eruptions are likely induced by these phenomena, a possible scenario for the future events.

1 Introduction

Awu is a little known active volcano located on Sangihe arc, northeast of Indonesia. It is the largest and the northernmost volcano of the arc with an aerial volume of $\sim 27 \text{ km}^3$ that constitutes the northern portion of Sangihe Island (Fig.1). The edifice culminates at 1318 m above sea level and extends nearly 2000 m to the sea bed, on its western flank. The summit crater is 1500 m in diameter and 380 m depth from the rim. It is currently occupied by a cooled lava dome. Since early 1980s, numerous studies have pointed to Awu as the center of strong volcanic manifestations with global impacts (Robock, 1981; 2000; Handler, 1984; Zielinski et al., 1994; Jones et al., 1995; Palmer et al., 2001; Donarummo et al., 2002; Guevra-Murua et al., 2015) although recent works have reviewed and declassified some of these events, including the 1641 event that was considered as responsible for 1642-1645 global cooling (e.g., Robock, 1981; Simkin et al., 1981; Jones et al., 1995) but later attributed to the Parker eruption of Jan. 4, 1641 (Delfin et al., 1997). Similarly, on the famous Edward Munch painting of 1893 - the “The Scream”, the red sky was first considered as induced by the 1892 eruption of Awu (Robock, 2000) but was later attributed to Krakatau 1883 eruption (Olson et al., 2004) and then finally considered



35 as inspired by the nacreous clouds (Fikke et al., 2017; Frata et al., 2018). But Awu 1812 eruption (VEI 4) has loaded a
significant amount of ash and aerosols into the atmosphere leading to the global abnormal correlation between dust load
in the atmosphere and solar activity (Donarummo et al., 2002). In 1856, another eruption on Awu (VEI 3) injected
massive sulfate aerosols into the stratosphere, leading to an increase of stratospheric aerosol's optical depth to 0.06,
sufficient to reduce the sea surface temperature and thus subsequently reducing the number of tropical cyclones
40 following the eruptive event (Guevara-Murua et al., 2015). In contrast, Handler (1984) indicates that the 1966 eruption
of Awu (VEI 4) loaded a notable amount of aerosols into the stratosphere resulting in a warmer eastern tropical Pacific
Ocean over three consecutive seasons with subsequent influence on El Nino type events. On the regional and local scale,
Awu eruptive activities have triggered at least two tsunamis, on Mar. 2, 1856 and on Jun. 7, 1892 (Latter et al., 1981;
Paris et al., 2014) with casualties. No less than 18 eruptions were reported on Awu volcano since 1640, thus about 1
45 eruption every ~20 years (Table 1). The latest eruption was a VEI 2 in 2004.

In the database of volcanic eruption victims compiled by Tanguy et al. (1998), Awu eruptions claimed a total of
5301 victims, mainly following lahar events, including 963 casualties during 1812 eruption, 2806 during 1856 eruption
and 1532 during 1892 eruption. This latter database did not take into account the 2508 victims of the 1711 eruption (Van
Padan, 1983, Data Dasar Gunung Api 2011). Around 3200 inhabitants were also reported killed by lahar events
50 following the 1822 eruption (Lagmay et al., 2007). The latest VEI 4 eruption on Awu in 1966 have killed 39 people,
injured 2000 and forced the evacuation of 420,000 inhabitants (Withan, 2005). In total since 1711, Awu recurrent
eruptive activities have caused a cumulative 11048 fatalities. Awu is thus one of the deadliest volcanoes worldwide but
paradoxically very little is known about its activity. This works aims to highlight the intense eruptive character of Awu
volcano and provide insights into the mechanism behind the recurrent energetic eruptions.

55

2 Methodology

The available documents that refer to Awu volcano, as summarized in the introduction, are generally incomplete but
most point to vigorous explosions and subsequent casualties. Thus to gain more insights into Awu's volcanic activity, a
60 reconnaissance visit to the summit was carried out in July 2015 with thermal and gas measurements. Thermal imaging
was performed using OPTRIS PI400, a miniature infrared camera that weighs 320g, including a lens of 62°x49° FOV,
f=8 mm and a dynamic range equivalent to the radiant temperature of -20°C to 900 °C. The detector has 382 × 288
pixels and the operating waveband is 7.5-13 μm. The maximum frame rate is 80 Hz. The camera was first positioned on
the crater rim (Fig.2) observing the whole crater, then in the crater, looking at the two main hot surfaces (Fig.2). The
65 radiant flux (Q_{rad}) estimation is obtained using the following: $Q_{\text{rad}} = A\epsilon\sigma(T_s^4 - T_a^4)$, where A is the hot surface, ϵ is the
emissivity (0.9 for andesite), σ is the Stefan-Boltzmann constant ($5.67 \times 10^{-8} \text{ W m}^{-2} \text{ K}^{-4}$), T_s is the hot surface temperature
and T_a is the ambient temperature. Thermal results are corrected for an oblique viewing angle of 30° following the
approach detailed in Harris (2013) and the hot surfaces in the crater are discriminated based on their brightness
temperature ranges, including 16-20 °C, 21-25 °C, 26-30 °C, 31-35 °C and 36-41 °C. Such thermal ranges allowed better
70 estimation of the total radiant flux given the heat distribution in the crater. Values below 16 °C fall in the background
level whilst 41 °C is the maximum temperature observed from the rim. Temperature values were corrected for



atmospheric influence relying on ACPC (<https://atmcorr.gsfc.nasa.gov/>) and validated with closer thermal recording before integrated into the radiant flux calculation. Thanks to the high acquisition rate of OPTRIS, few series of continuous recordings were obtained on the most heated surfaces to retrieve the heat flow dynamic.

75 A portable Multi-GAS system from INGV (as used by Aiuppa et al. 2015; Bani et al., 2017; 2018) was deployed to measure the gas composition. The instrument was positioned at different locations in the crater (Fig.2) and simultaneously acquired concentrations of H₂O, CO₂, SO₂, H₂S, and H₂ at 0.1 Hz. Data were processed using Ratiocalc (Tamburello 2015). The scanning DOAS was used for the gas emission budget. The instrument performed at fixed position in the crater (Fig.2). Further details on this Awu's gas measurement are provided in a separate paper and
80 hereafter referred to as (Bani et al. submitted).

The lava dome was sampled during this fieldwork then analyzed for major and trace elements using ICP-AES.

3 Results

The whole-rock composition of the lava dome, obtained from ICP AES analysis, indicates a source with 52-56% SiO₂ and relatively low alkaline corresponding to basaltic-andesite melt source (Table 2, Fig.3). Results are comparable with
85 the data from Morrice et al (1983) and Hanyu et al. (2012). Trace elements normalized to N-MORB point out elevated ratios of large ion lithophile elements (LILEs), light rare elements (LREEs) and high-field strength elements (HFSEs) (Table 2, Fig.3).

DOAS measurement results obtained on Awu indicate a relatively small degassing with a mean daily SO₂ emission rate
90 of 13±6 tons. The multigas results indicate H₂S/SO₂, CO₂/SO₂, H₂/SO₂ and H₂O/SO₂ ratios of 49, 297, 0.1 and 1596 respectively with the corresponding gas composition equivalent to 82% of H₂O, 15% of CO₂, 2% of H₂S, 0.05% of SO₂ and 0.02% of H₂. Assuming the above results are representative then H₂O, CO₂, H₂S, and H₂ emission rates would be 5800 t/d, 2600 t/d, 340 t/d and 0.1 t/d respectively. The gas equilibrium temperature obtained by resolving together the SO₂/H₂S vs. H₂/H₂O redox equilibria (see methodology in Aiuppa et al., 2011; Moussallam et al., 2017) is circa 380 °C
95 (Bani et al., submitted)

Thermal infrared recording from the rim highlights two main heated surfaces in Awu's crater, but both are located to the northern part of the lower crater wall, next to the lava dome (IR2, IR3, Fig.3). It is also evident from these thermal results that the lower crater wall around the dome is much hotter than the lava dome itself. The total radiant flux from the crater (IR1, Table 4) is 27±12 MW, including 5.6±2.4 MW from the lava dome and 21±9 MW from the area surrounding
100 the dome. The highest radiant flux per area (0.9 MW) is recorded in the IR3 zone where gas is released at a low frequency of 0.3 Hz with a thermal fluctuation amplitude of 0.1-0.3 MW.

4 Discussion

4.1 Melt source

105 To sustain the recurrent strong eruptive activity on Awu, highlighted by one strong eruption every 20 years over the last 3.5 centuries (including two VEI 4 and three VEI 3), it requires sufficient magma supply rate. The alkaline vs. SiO₂ diagram (Table 2., Fig.3) indicates a basaltic andesite melt composition typical of island arc volcanoes where the geodynamic context allows a relatively evolved source. Awu is part of Sangihe arc where the geodynamic processes are



controlled by the divergent double subduction that the currently resulted in Sangihe forearc overriding the Halmahera
110 forearc (Cardwell et al., 1980, Morrice et al., 1983, Hall and Wilson, 2000; Jaffe et al., 2004; Zhang et al., 2017; Bani et
al., 2018). The pattern obtained by normalizing the trace elements to N-MORB indicates high LILE (Cs, K, Rb, Ba and
Sr) content and low abundance of HFSE, represented by Nb, typical of subduction melt source in which the mantle
wedge has been contaminated by fluid released from the subduction slab (McCulloch and Gambke, 1991; Davidson
1996, Mcpherson et al., 2003). This result is coherent with Jaffe et al. (2004) who highlight low $^3\text{He}/^4\text{He}$ (5.4-6.4 R_A) and
115 high $\text{CO}_2/^3\text{He}$ ratios (64-180 $\times 10^9$) as well as high $\delta^{13}\text{C}$ ($\geq -2\text{‰}$) suggesting slab contribution into the magmatic fluids at
Awu. Clor et al. (2005) further point out anomalous high N_2/He (2852) coupled with low $\delta^{15}\text{N}$ (3.3%) suggesting
increased slab contribution, possibly by slab melting as collision stalls the progress of the subducting plate and allows it
to become superheated (Peacock et al., 1994). This is supported by the slow-down of the subduction rate as evidenced by
seismic studies (McCaffrey, 1983; Pubellier et al., 1991; Zhang et al., 2017). This particular double subduction and arc-
120 arc collision have rendered the slab prone to melting that subsequently produces the magmatic source behind the
recurrent strong eruptive activities on Awu. The mechanism also contributes to unusual slab carbon delivery into the
mantle as highlighted by the extremely elevated CO_2 (Bani et al. submitted).

4.2 A conduit plug

125 Lava domes are formed when viscous lava extruded to the surface effusively then pile up around the vent. Such
phenomena involve complex processes, including crystallization, bubble nucleation, growth, coalescence and out-
gassing, bulk magma deformation, crack propagation and healing (e.g., Ashell et al., 2015 and ref therein). It is the
competition between these processes that either promote or prevent degassing, leading to explosions or stability of a lava
dome (Klug and Cashmana, 1996; Takeuchi et al., 2005; Mueller et al., 2008). On Awu, the SiO_2 content of the lava
130 dome higher than 50 wt% as well as the perfect semi-spherical morphology of $\sim 1.3 \times 10^7 \text{ m}^3$ that extended from the
middle of the crater suggests an endogenous growth that generally inflates the dome carapace through magma injection
at depth. In such case, lava domes are known to induce variable porous and brecciated carapace surrounding a denser
and coherent interior (Fink et al., 1992; Wadged et al., 2009, Ashell et al., 2015; Newhall and Melson, 1983) suitable to
form a plug in the upper conduit (Watts et al. 2002). The radiant thermal energy around the lava dome is much higher
135 than the heat release from the dome representing 79% of the total 27 MW from the crater. Only ~ 6 MW is released
through the lava dome itself. It also around the dome that much of the gas is released to the atmosphere (Figure 5). The
hottest surfaces also correspond to the main degassing points which suggest that heat is rather sustained by fluid
circulations around the dome. With a conduit plug, the gas released at depth is thus forced to the periphery of the lava
dome (Fig.5), similar to other dome-forming systems, including Rokatenda (Primulyana et al., 2018), Lascar (Matthews
140 et al., 1997) or Soufriere Hills (Sparks, 2003).

It is thus obvious that the existence of a conduit plug may constitute a barrier to the gas flow, suitable for rapid pressure
built up with new magma injection, a situation that can strongly contribute to the vigorous explosions on Awu.



145 **4.3 Transition of heat to the surface controls the water accumulation**

Out of the 17 recorded eruptive activities on Awu, 11 were tagged as phreatic and 6 other eruptions were phreatomagmatic (Table 1). It is thus unambiguous that water played a major role in Awu volcanic activity. Indeed, with an average annual rainfall of 3500 mm (Stone, 2010) and a crater area of 1.5 km², the Awu summit is likely to accommodate 5.2x10⁶ m³ of water each year. Given that there is no visible water outlet from the crater, one can expect water accumulation and strong infiltration into the hydrothermal system which may then subsequently contribute to phreatic eruptions. But as highlighted in figure 6, surface water was not always present in Awu's crater. Crater lake existed in 1922, 1973 and 1995 whilst in 1931 and 1979 crater lake co-existed with a lava dome. In July 2015 (this fieldwork) there was no water in the crater and a lava dome occupied the central part of the crater. July is among the driest month of the year, however, the average monthly rainfall on Sangihe Island doesn't fall below 130 mm (Stone, 2010). Hence one can expect a cumulative water volume of at least 195x10³ m³ (equivalent to 7x10⁶ moles or 1.3x10⁸ g, using PV=nRT) into Awu's crater on that period of the year. But the absence of water as observed in July indicate that the water was efficiently infiltrated and evaporated away. In theory, if we assume that the infiltration is negligible, then it requires a heat energy of 8.0x10¹¹ joules (using mC_pΔT; m is the water mass, C_p is the water's specific heat capacity, ΔT is the difference between boiling and ambient temperature) to bring the above volume to the evaporation temperature (100°C) and another 4.6x10⁹ joules (using mL; L is the latent heat of vaporization) to convert it into water vapor. A total 8.1x10¹¹ joules is thus sufficient to dry out the July incoming water volume. With 27 MW of radiant flux from the crater, equivalent to 2.7x10⁷ J s⁻¹, only 8 hours is necessary to heat the 7x10⁶ moles of water from 16 °C to the evaporation temperature and transform it to water vapor. This duration should be considered maximum as the portion of water infiltration is ignored. Nevertheless, the above simple calculation suggests that the heat transfer to the surface from the magmatic source is largely sufficient to evaporate out the water and thus controlling the water accumulation in Awu's crater. This is coherent with the 95% water loss by evaporation from the 3.5x10⁶ m³ of the lake volume before to the 1992 eruption (Table 1). Similarly, in 2004 the lake water progressive dried out before the eruption. But if that the cooling trend in the crater continues, then ultimately the heat will no longer sufficient to dry out the incoming water from the rainfall. Water may then accumulate to form a crater lake as already observed in the past.

170

4.4 The Hazardous situation

The contact of liquid water with a hot surface is widely accepted as a process that can trigger explosive water-magma interactions (Wohletz, 1986; 2002; Zimanowski et al., 1995; Thiéry and Mercury, 2009). However, according to a review of historical eruptions through volcanic lakes, ~2% involved relatively passive growth of subaqueous to emergent lava domes (Manville, 2015). This was the case on Kelud volcano (Java) in 2007 where a lava dome emerged in the middle of a huge crater lake without any vigorous explosion as suspected (Hidiyati et al., 2009). But only 7 years later, in 2014 that a VEI 4 eruption was witnessed on the volcano (Kristiansen et al., 2014). On Awu given the limited information on its past activities, it is difficult to provide a rigorous description of the successive lava dome emplacement. However, the coexistence of lava dome and crater lake in 1931 and 1979 were preceded by crater lake solely and no eruption in between (Fig.6). Such sequence suggests that Awu lava domes possibly occurred through the crater lake without explosive water-magma interactions. Further, the cooling and the relatively small and steady volume

180



of Awu's lava dome on a flat crater floor represent less probability for a dome collapse, contrasting with other domes
were the average rate of dome growth is approximately $10^4 \text{ m}^3 \text{ day}^{-1}$ with a mean volume of $5 \times 10^7 \text{ m}^3$ and some with
unstable slopes (Newhall and Melson, 1983). The hazardous situation on Awu is thus more related to the presence of the
185 conduit plug and a crater lake since this latter may further increase the potential of violent eruptions (Sheridan and
Wohletz 1983; Wohletz 1986). Similar to Kelud 2014 eruption, the vigorous VEI 4 eruption witnessed on Awu in 1966
occurred 35 years following the lava dome emplacement. Also, the 1992 eruption has pulverized a lava dome formed 13
years earlier. The current lava dome on Awu has developed 16 years ago, just after the 2004 eruption. The prevalence of
 H_2S over SO_2 , the low SO_2 emission budget of 13 t/d and the low equilibrium temperature of circa $380 \text{ }^\circ\text{C}$ obtained by
190 resolving together the $\text{SO}_2/\text{H}_2\text{S}$ vs. $\text{H}_2/\text{H}_2\text{O}$ redox equilibria (see methodology in Aiuppa et al., 2011; Moussallam et al.,
2017) indicate that the current activity on Awu is sustained by a degassed magma. Hence, assuming that the processes
that lead to vigorous eruption will repeat themselves then the subsurface volcanic system has to develop more than 3.1
MPa of pressure (Pressure (Pa) = F/Area (m^2); F (N) = masse (kg) x $9.8 \text{ (m/s}^2\text{)}$; density of 2700 kg/m^3) to destabilized the
 $3.5 \times 10^{10} \text{ kg}$ of lava dome. The total pressure than can be developed in the conduit or reservoir generally reaches tens of
195 magapascals (e.g., Gudmundsson, 2012), largely sufficient to clear-up the conduit and pulverize the lava dome. Thus a
new magma injection into the reservoir may be necessary to induce a rapid pressure buildup, capable to pulverize the
lava dome and the conduit plug. This latter scenario may constitute an opening phase of volcanic eruption, creating a
favorable condition for a rapid external lake water injection that could lead to magma-water interaction. Events of
particularly high intensity described as phreato-Plinian eruptions can only be explained with the involvement of surface
200 water in the eruption dynamics (Areva et al., 2018). A presence of water in Awu's crater may thus increase the potential
of intense eruptive manifestations, a possible scenario behind the past vigorous eruptions. The most hazardous situation
on the Awu volcano would be the new magma injection into the reservoir beneath a conduit plug and a sufficient water
volume in the crater lake (Fig.7).

205 **5 Conclusion**

Awu is the northernmost active volcano of the Sangihe arc with 18 eruptions over the last 3.5 centuries,
including 2 with VEI 4 and 3 with VEI 3 with local, regional and even worldwide impacts. Awu is also one of the
deadliest volcano on earth with a cumulative dead toll of 11048 following its recurrent eruptive activity. Paradoxically,
very little is known about this volcano. As emphasized in this work, the regular magma supply that sustained the activity
210 of Awu is possibly linked to the peculiar geodynamic context of the region, controlled by the divergent double
subduction and the subsequent arc-arc collision. Awu also has the particularity to host alternatively or simultaneously a
lava dome and a crater lake. Lava domes at Awu seem to occur passively through crater lake and the heat that
accompanied this emplacement has shown to be sufficient to dry out the water. The emplacement of the lava domes also
appears to be associated with a conduit plug development that forces the degassing to the crater wall. With time the lava
215 dome cools down, allowing progressively the crater lake formation with the high annual rainfall in the region. This
scenario may ultimately constitute the most hazardous situation if a new magma injection occurs at deep. Indeed this
latter may induce a rapid pressure buildup that can pulverize the conduit plug and the lava dome, creating a favorable
condition for large water injection and a subsequent explosive water-magma interaction. Such a scenario likely resulted



220 in the past vigorous eruptions on Awu and may occur in the future given the presence of a cooling lava dome and a
conduit plug.

Acknowledgments

225 This work was supported by IRD under the JEAI-COMMISSION program in collaboration with CVGHM. Sincere
acknowledgment to pak Endi and the other staffs of Awu observatory for their support in organizing the expedition to the
crater of Awu.

References

- Aiuppa, A., Shinohara, H., Tamburello, G., Giudice, G., Liuzzo, M., Moretti, R.: Hydrogen in the gas plume of an open-vent volcano, Mount Etna, Italy. *J. Geophys. Res. B: Solid Earth* 116 (10), B10204, 2011.
- Aiuppa, A., Bani, P., Moussallam, Y., Di Napoli, R., Allard, P., Gunawan, H., Hendrasto, M., Tamburello, G.: First determination of magmaderived gas emissions from Bromo volcano, eastern Java (Indonesia). *J Volcanol Geotherm Res* 304:206–213. <https://doi.org/10.1016/j.jvolgeores.2015.09.008>, 2015.
- Aravena, A., de' Michieli Vitturi, M., Cioni, R., and Neri, A.: Physical constraints for effective magma-water interaction along volcanic conduits during silicic explosive eruptions: *Geology*, v. 46, p. 867–870, <https://doi.org/10.1130/G45065.1.1>, 2018.
- Ashwell, P. A., Kendrick, J. E., Lavallée, Y., Kennedy, B. M., Hess, K.-U., von Aulock, F. W., Wadsworth, F. B., Vasseur, J., Dingwell, D. B.: Permeability of compacting porous lavas. *J. Geophys. Res. Solid Earth*, 120, 1605-1622, [doi:10.1002/2014JB011519](https://doi.org/10.1002/2014JB011519), 2015.
- Bani, P., Alfianti, H., Aiuppa, A., Oppenheimer, C., Sitingjak, P., Tsanev, V., Saing, U. B.: First study of heat and gas budget for Sirung volcano, Indonesia. *Bull Volcanol* 79(8):60. <https://doi.org/10.1007/s00445-017-1142-8>, 2017.
- Bani, P., Tamburello, G., Rose-Koga, E. F., Liuzzo M., Aiuppa, A., Cluzel, N., Amat, I., Syahbana, D. K., Gunawan, H.: Dukono, the predominant source of volcanic degassing in Indonesia, sustained by a depleted Indian-MORB. *Bull. Volcanol.*80:5. <https://doi.org/10.1007/s00445-017-1178-9>, 2018.
- Cardwell, R. K., Isacks, B. L., Karig, D. E.: The spatial distribution of earthquakes, focal mechanism solutions and subducted lithosphere in the Philippine and northeast Indonesian islands. *Am Geophys Union Geophys Monogr* 23:1–36, 1980.
- Data Dasar Gunung Api, Wilaya Timur: edisi kedua. Kementerian Energi dan Sumber Daya Mineral, Badan Geologi, pp. 1-450, 2011.
- Davidson, J. P.: Deciphering mantle and crustal signatures in subduction zones. In: Bebout G E, Scholl D W, Kirby S H, Platt J P (eds) *Subduction: top to bottom*, vol 96. American Geophysical Union Monograph, pp 251–262, 1996.
- Delfin, F. G., Newhall, C. G., Martinez, M. L., Salonga, N. D., Bayon, F. E. B., Trimble, D., and Solidum, R.: Geological, ^{14}C and historical evidence for a 17th century eruption of Parker volcano, Mindanao, Philippines, *J. Geol. Soc. Philipp.*, 52, 25-42, 1997.
- Donarummo Jr., J., Ram, M., Stolz, M. R.: Sun/dust correlations and volcanic interference. *Geophys. Res. Lett.*, 29, No 9, 1361, [doi:10.1029/2002GL014858](https://doi.org/10.1029/2002GL014858), 2002.



- Fikke, S. M., Kristjánsson, J. E., Nordli, O.: Screaming clouds. *Weather*, 72, 115–121, <https://doi.org/10.1002/wea.2786>, 2017.
- Fink, J. H., Anderson, S. W., Manley, C. R.: Textural constraints on effusive silicic volcanism: Beyond the permeable foam model, *J. Geophys. Res.*, 97(B6), 9073–9083, doi:10.1029/92JB00416, 1992.
- Global Volcanism Program: Awu (267040) in *Volcanoes of the World*, v. 4.8.5. Venzke, E (ed.). Smithsonian Institution. Downloaded 11 Jan 2020 (<https://volcano.si.edu/volcano.cfm?vn=267040>). <https://doi.org/10.5479/si.GVP.VOTW4-2013>, 2013.
- Gudmundsson, A.: Magma chambers: Formation, local stresses, excess pressures, and compartments. *J. Volcanol. Geotherm. Res.*, 237-238, 19-41, 2012.
- Guevara-Murua, A., Henty, E. J., Rust, A. C., Cashman, K. V.: Consistent decrease in North Atlantic Tropical Cyclone frequency following major volcanic eruption in the last three centuries. *Geophys. Res. Lett.*, 42, 9425–9432, doi:10.1002/2015GL066154, 2015.
- Hall, R., Wilson, M. E. J.: Neogene sutures in eastern Indonesia. *J Asian Earth Sci* 18:781–808, 2000.
- Handler P.: Possible association of stratospheric aerosols and El Nino type events. *Geophys. Res. Lett.*, 11, 1121-1124, 1984.
- Hanyu, T., Gill, J., Tatsumi, Y. et al.: Across- and along-arc geochemical variations of lava chemistry in the Sangihe arc: Various fluid and melt slab fluxes in response to slab temperature, *Geochem. Geophys. Geosyst.*, 13, Q10021, doi:10.1029/2012GC004346, 2012.
- Harris, A.: *Thermal Remote Sensing of Active Volcanoes, A user's Manual*. Cambridge University Press, UK, pp. 1-728, 2013.
- Hidayati, S., Basuki, A., Kristianto, Mulyana, I.: Emergence of Lava Dome from the Crater Lake of Kelud Volcano, East Java. *J. Geologi Indonesia*, 4, 229-238, 2009.
- Jaffe, L. A., Hilton, D. R., Fisher, T. P., Hartono, U.: Tracing magma sources in an arc-arc colliding zone: Helium and carbon isotope and relative abundance systematic of the Sangihe Arc, Indonesia. *Geochem. Geophys. Geosyst.*, 5, Q04J10, doi:10.1029/2003GC000660, 2004.
- Jones, P. D., Briffa, K. R., Schweingruber, F. H.: Tree-ring evidence of the widespread effects of explosive volcanic eruption. *Geophys. Res. Lett.*, 22, 1333-1336, 1995.
- Kristiansen, N. I., Prata, A. J., Stohl, A., and Carn, S. A.: Stratospheric volcanic ash emissions from the 13 February 2014 Kelut eruption, *Geophys. Res. Lett.*, 42, 588–596, doi:10.1002/2014GL062307, 2015.
- Lagmay, A. M. F., Rodolfo, K. S., Siringan, F. P., Uy, H., Remotigue, C., Zamora, P., Lapus, M., Rodolfo, R., Ong, J.: Geology and hazard implications of the Maraunot notch in the Pinatubo Caldera, Philippines. *Bull. Volcanol.*, 69, 797-809, 2007.
- Latter, J. H.: Tsunamis of Volcanic Origin: Summary of Causes, with Particular Reference to Krakatoa, 1883. *Bull. Volcanol.*, 43-3, 1981.
- Macpherson, C. G., Forde, E. J., Hall, R., Thirlwall, M. F. Geochemical evolution of magmatism in an arc-arc collision: the Halmahera and Sangihe arcs, eastern Indonesia. In: Larter RD, Leat PT (eds) *Intraoceanic Subduction systems: tectonic and magmatic processes*, vol 219. Geological Society, London, Special Publications, pp 207–220. <https://doi.org/10.1144/GSL.SP.2003.219.01.10>, 2003.



- McCaffrey, R.: Seismic-wave propagation beneath the Molucca Sea arc-arc collision zone, Indonesia, *Tectonophysics*, 96(1–2), 45–57, doi:10.1016/0040-1951(83)90243-3, 1983.
- McCulloch, M. T., Gamble, J. A.: Geochemical and geodynamical constraints on subduction zone magmatism. *Earth Planet Sci Lett* 102(3-4):358–374. [https://doi.org/10.1016/0012-821X\(91\)90029-H](https://doi.org/10.1016/0012-821X(91)90029-H), 1991.
- Morrice, M. G., Jezek, P. A., Gill, J. B., Withford, D.J., Monoarfa, M.: An introduction to the Sangihe arc: volcanism accompanying arc-arc collision in the Molucca sea, Indonesia. *J. Volcanol. Geotherm. Res.*, 19, 135-165. Newhall, C. G., Melson, W. G, 1983. Explosive activity associated with the growth of volcanic domes. *J. volcanol. Geotherm Res.*, 17, 111-131, 1983.
- Olson, D. W., Doescher, R. L., Olson, M. S.: When the sky ran red: The story behind “the Scream”. *Sky and Telescope*, 28-35, 2004.
- Palmer, A. S., van Ommen, T. D., Curran, M. A. J., Morgan, V., Souney, J. M., Mayewski, P. A.: High-precision dating of volcanic events (A.D. 1301-1995) using ice cores from Law Dom, Antarctica. *J. Geophys. Res.*, 106, 28089-28095, 2001.
- Paris, R., Switzer, A. D., Belousova, M., Belousov, A., Ontowirjo, B., Whelley, P. L., Ulvrova, M.: Volcanic tsunamis: a review of source mechanisms, past events and hazards in Southeast Asia (Indonesia, Philippines, Papua New Guinea). *Nat. Hazards*, 70:447-470, doi:10.1007/s11069-013-0822-8, 2014.
- Prata, F., Robock, A., Hamblyn, R.: The Sky in Edvard Munch’s The Scream. <https://doi.org/10.1175/BAMS-D-17-0144.1>, 2018.
- Klug, C., Cashman, K. V.: Permeability development in vesiculating magmas: Implications for fragmentation, *Bull. Volcanol.*, 58, 87–100, 1996.
- Manville, V.: Volcano-Hydrologic hazards from Volcanic Lakes. In Rouet, D., Christensen, B., Tassi, F., Vandemeulebrouck (eds), *Volcanic Lakes, Advances in Volcanology*, DOI 10.1007/978-3-642-36833-2_2, 2015.
- Matthews, S. J., Gardeweg, M. C., Sparks. R. S. J.: The 1984 to 1996 cyclic activity of Lascar Volcano, northern Chile: cycles of dome growth, dome subsidence, degassing and explosive eruptions. *Bull Volcanol*, 59(1):72–82, 1997.
- Moussallam Y., Peters, N., Masias, P., Aaza, F., Barnie, T., Schipper, C. I., Curtis, A., Tamburello, G., Aiuppa, A., Bani, P., Giudice, G., Pieri, D., Davies, A. G., Oppenheimer, C.: Magmatic gas percolation through the old lava dome of El Misti volcano. *Bull. Volcanol.* 79:46, doi: 10.1007/s00445-017-1129-5, 2017.
- Mueller, S., Scheu, B., Spieler, O., Dingwell, D. B.: Permeability control on magma fragmentation, *Geology*, 36(5), 399–402, 2008.
- Primulyana, S., Bani, P., Harris, A.: The effusive-explosive transitions at Rokatenda 2012-2013; unloading by extrusion of degassed magma with lateral gas flow. *Bull Volcanol*, 79:22, doi 10.1007/s00445-07-1104-1, 2017.
- Robock, A.: A latitudinally dependent volcanic dust veil index, and its effect on climate simulations. *J. Volcanol. Geotherm. Res.* 11, 67-80, 1991.
- Robock, A.: Volcanic eruptions and climate. *Rev. Geophys.*, 38, 191-219, 2000.
- Siebert, L., Simkin, T., Kimberly, P.: *Volcanoes of the World*, third edition, University of California Press, pp. 1-155, 2010.



- Sheridan, M. F., Wohletz, K. H.: 1983. Hydrovolcanism: basic considerations and review. *J. Volcanol. Geotherm. Res.* 17:1-29, 1983. Simkin, T. P., Siebert, L., McClelland, L., Bridge, D., Newhall, C., Latter, J. H.: *Volcanoes of the World*, Hutchinson-Ross, Stroudsburg, 1981.
- Sparks, R. S. J.: Dynamics of magma degassing. In: Oppenheimer, C., Pyle, D. M., Barclay, J., (eds) *Volcanic Degassing*. Geol. Soc. Lond., Spec. Publ. 213:5–22, 2003.
- Stone, M.: Independent Technical Report, Sangihe Property, Sangihe Island, North Sulawesi, Indonesia. Toronto, Ontario, pp. 1-130, 2010.
- Takeuchi, S., Nakashima, S., Tomiya, A., Shinohara, H.: Experimental constraints on the low gas permeability of vesicular magma during decompression, *Geophys. Res. Lett.*, 32, L10312, doi:10.1029/2005GL022491, 2005.
- Tamburello, G.: Ratiocalc: software for processing data from multicomponent volcanic gas analyzers. *Comput. Geosci.* 82:63–67. <https://doi.org/10.1016/j.cageo.2015.05.004>, 2015.
- Tanguy, J.-C., Ribiere, C., Scarth, A., Tjetjep, W. S.: Victims from volcanic eruptions: a revised database. *Bull. Volcanol.*, 60, 137-144, 1998.
- Thiéry, R., Mercury, L.: Explosive properties of water in volcanic and hydrothermal systems. *J. Geophys. Res.*, 114, B05205, doi:10.1029/2008JB005742, 2009.
- Van Padang, N.: History of volcanology in the East Indies, *Scripta Geol.*, 71, 1983.
- Wadge, G., Ryan, G., Calder, E.S.: Clastic and core lava components of a silicic lava dome, *Geology*, 37(6), 551–554, 2009.
- Watts, R. B., Herd, R. A., Sparks, R. S. J., Young, S. R.: Growth patterns and emplacement of the andesite lava dome at Soufrière Hills Volcano, Montserrat. In: Dritt, T. H., Kokelaar, B. P. (eds), *The Eruption of Soufrière Hills Volcano, Montserrat, from 1995 to 1999*. Geological Society, London, Memoirs, 21, 115–112, 2002.
- Wichmann, A.: Über den Ausbruch des Gunung Awu am 7. Juni 1892. *German Journal of Geology*, 3, 543-546, 1893.
- Witham, C. S.: Volcanic disasters and incidents: A new database. *J. Volcanol. Geotherm. Res.* 148, 191-233, 2005.
- Wohletz, K.: Explosive magma-water interactions: Thermodynamics, explosion mechanisms, and field studies, *Bull. Volcanol.*, 48, 245–264, 1986.
- Wohletz, K.: Water/magma interaction: Some theory and experiments on peperite formation, *J. Volcanol. Geotherm. Res.*, 114, 19–35, 2002.
- Zhang, Q., Guo, F., Zhao, L., Wu, Y.: Geodynamics of divergent double subduction: 3-D numerical modeling of a Cenozoic example in the Molucca Sea region, Indonesia. *J. Geophys. Res. Solid Earth*, 122, 3977-3998, doi:10.1002/2017JB013991, 2017.
- Zielinski, G. A., Fiacco, R. J., Whitlow, S., Twickler, M. S., Germani, M. S., Endo, K., and Yasui, M.: Climatic impact of the AD 1783 eruption of Asama (Japan) was minimal: evidence from the GISP2 ice core. *Geophys. Res. Lett.* 21, 2365-2368, 1994.
- Zimanowski, B., Frohlich, G., and Lorenz, V.: Experiments on steam explosion by interaction of water with silicate melts, *Nucl. Eng. Des.*, 155, 335–343, 1995.



Captions

Table 1. History of Awu eruptive activity. Most of the information is obtained from Data Dasar, Gunung Api, (2011) and Siebert et al. (2010).

Date	Eruptive events
1640 (Dec.)	Phreatic eruption (Data Dasar, Gunung Api, 2011; Siebert et al., 2010).
1641 (Jan.3-4)	Phreatic eruption, lahar event (Wichmann, A., 1893; Siebert et al., 2010; Data Dasar, Gunung Api, 2011).
1677	Phreatic eruption (Data Dasar, Gunung Api, 2011).
1711 (Dec. 10-16)	On the night of Dec. 10, violent eruption (VEI 3) propelled incandescent material above the summit. Pyroclastic flow combined with hot lahar, generated by the outburst of the crater lake, wiped out the entire city of Kandhar located at the eastern base of the edifice. About 3000 people were killed, including 2030 in Kendhar and 408 at Tahuna. Among those victims, 400 corpses were described as suffocated by the heat of pyroclastic (Wichmann, A., 1893; Van Padang, 1983; Data Dasar, Gunung Api, 2011; Siebert et al., 2010).
1812 (Aug. 6-8)	Large phreatomagmatic eruption (VEI 4) with manifestations comparable to the 1711 event. Lahar and pyroclastic flows have destroyed villages, destroying all the coconut trees along the coast. 963 inhabitants were killed, particularly in the village of Tabuhan, Khendar and Kolengan (Tanguy et al., 1998; Data Dasar, Gunung Api, 2011).
1856 (Mar. 2-7)	Large phreatomagmatic eruption (VEI 3) with associated pyroclastic and lahar flow that killed 2806 inhabitants. The eruption has also triggered a tsunami event (Wichmann, A., 1893; Siebert et al., 2010, Tanguy et al., 1998).
1875 (Aug.)	Phreatic eruption (VEI 2) with no further report (Siebert et al., 2010; Data Dasar, Gunung Api, 2011).
1883 (Aug. 25-26)	Eruption (VEI 2) but no further detail (Siebert et al., 2010).
1885 (Aug. 18)	Phreatic eruption (VEI 2) but no further detail (Siebert et al., 2010; Data Dasar, Gunung Api, 2011).
1892 (Jun. 7-12)	Large phreatomagmatic eruption (VEI 3). Beginning at 6:10 am – then a huge column was seen ascending into the atmosphere in the afternoon, accompanied by lightning and thunderstorms. Muddy rain turned into pumice and heavy ashfall when the eruption reached the climax of its violence at 9 pm with pyroclastic flow and lahar before it started to fade after midnight. A large number of huts collapsed under the weight of ash and extensive mudflow occurred during and following the event. The eruption has also triggered a Tsunami event. 1532 inhabitants were reported killed, mainly by Pyroclastic and lahar events in many areas, including Mala, Akembuala, Anggis, Mitung, Kolengan, Metih, Khendar and Trijang. Many victims are killed while in church buildings (Wichmann, A., 1893; Van Padang, 1983; Data Dasar, Gunung Api, 2011; Tanguy et al., 1998).



1893	Phreatic eruption (VEI 2) but no further detail (Data Dasar, Gunung Api, 2011; Siebert et al., 2010).
1913 (Mar. 14)	Phreatic eruption (VEI 2) (Data Dasar, Gunung Api, 2011; Siebert et al., 2010).
1921 (Feb.)	Phreatic eruption (VEI 0) – crater lake activity (Data Dasar, Gunung Api, 2011; Siebert et al., 2010).
1922 (Jun.-Sep.)	Phreatic eruption (VEI 0) - crater lake activity (Data Dasar, Gunung Api, 2011; Siebert et al., 2010).
1931 (Apr.-Dec.)	Lava dome started to form in the crater lake in April and then progressively grew until reaching 80 m above the water in Dec. (Data Dasar, Gunung Api, 2011).
1966 (Aug. 12)	At 8:20 (Aug.12), a VEI 4 began with a sudden thick smoke that rose from the crater associated with a strong blast. An hour later another strong blast occurred propelling voluminous amount of ash that subsequently blanketed the summit. Other strong explosions followed until around 13:30 and pyroclastic flow extended 5 km from the crater. Lahars have traveled 7 km toward the coast. along the water channels. Both phenomena have destroyed everything in their respective passages. Kendhar and Mala were the most affected area with 13 and 18 casualties respectively. Eight other inhabitants were also killed in other areas, including 2 officials. In total, the eruption killed 39 and caused the displacement of 11000 inhabitants (Data Dasar, Gunung Api, 2011; Siebert et al., 2010).
1992 (May-Oct. 12)	Phreatic eruption (VEI 1). Before the eruption, the lake volume decreased by 95% from the initial $3.5 \times 10^6 \text{ m}^3$ of water. On Oct. 12, a phreatic eruption occurred (Data Dasar, Gunung Api, 2011; Siebert et al., 2010).
2004 (Jun. 8-10)	Magmatic eruption (VEI 2) building a column of 1000-3000 meters above the crater. The resulting ashfall extended kilometers from the volcano. At Tabukan, 15 km southeast of the volcano the ash was 0.5-1 mm thick. 18648 people were displaced but no one was killed (Data Dasar, Gunung Api, 2011; Siebert et al., 2010).



Table 2. Major and trace composition of Awu lava dome.

	S1 (lava dome)	S2 (lava dome)	S3* (volc. rock)	S4* (south Sangihe Is.)	S5**	S5**
SiO₂ (wt%)	53.95	54.10	52.27	58.50	55.11	54.54
TiO₂	0.77	0.71	0.72	0.61	0.69	0.73
Al₂O₃	18.40	18.90	18.44	18.26	18.73	18.68
Fe₂O₃	8.85	8.60	8.20	7.47	8.53	8.52
MnO	0.21	0.20	0.19	0.16	0.19	0.19
MgO	3.79	3.61	3.44	2.61	3.34	3.42
CaO	8.73	8.85	8.42	7.16	7.76	8.60
Na₂O	3.70	3.53	3.91	3.51	3.52	3.51
K₂O	1.17	1.13	1.21	1.50	1.40	1.21
P₂O₅	0.19	0.16	0.19	0.22	0.22	0.19
LOI	0.30	0.0	0.34	0.94		
Total	99.75	99.83	98.69	100.65	99.49	99.59
Ba (ppm)	227	230	228	214	272	226
Sr	378	378	373	431	419	366
Rb		19	20	30	25.5	19.80
Cs			1.0	0.7	1.00	1.01
Y		23.3	26	51	18.8	20.5
Zr		70.7	74	107	72.8	72.0
Ni		5.4	<5	<5		
Sc		22.4				
V		242.5				
Cr		4.9				
Co		19.4				
Nb		2.6			3.04	2.17
La		4.9			7.25	5.95
Ce		13.8			16.4	14.80
Nd		8.7			10.8	10.30
Sm		2.3			2.90	2.95
Eu		0.72			0.97	1.01
Gd		2.7			3.20	3.45
Dy		2.8			3.43	3.80
Er		1.7			2.20	2.5
Yb		1.92			2.20	2.48
Th		0.4			1.33	1.10

* data from Morrice et al. (1983); ** data from Hanyu et al. (2012).



Table 3. Thermal radiant flux from Awu crater

Surface (m ²)	IR1	IR2	IR3	Dome	
92681	1852	1631	13225		
Temp. range	Corrected mean temp. (°)	Surface occupied per temperature range (%)			
16-20 °C*	93.4	51.8	54.2	51.3	78
21-25 °C	97.3	1.1	27.9	13.9	0.5
26-30 °C	101.2	0.4	11.4	13.5	0.1
31-35 °C	105.3	0.3	6.5	14.3	0
36-41 °C	109.8	0.1	0	2.9	0
Mean Radiant flux (MW)	27 ± 12	0.5 ± 0.2	0.9 ± 0.3	5.6 ± 2.4	

* Note that below 16°C, it was difficult to discriminate the heated zones from the background surface.

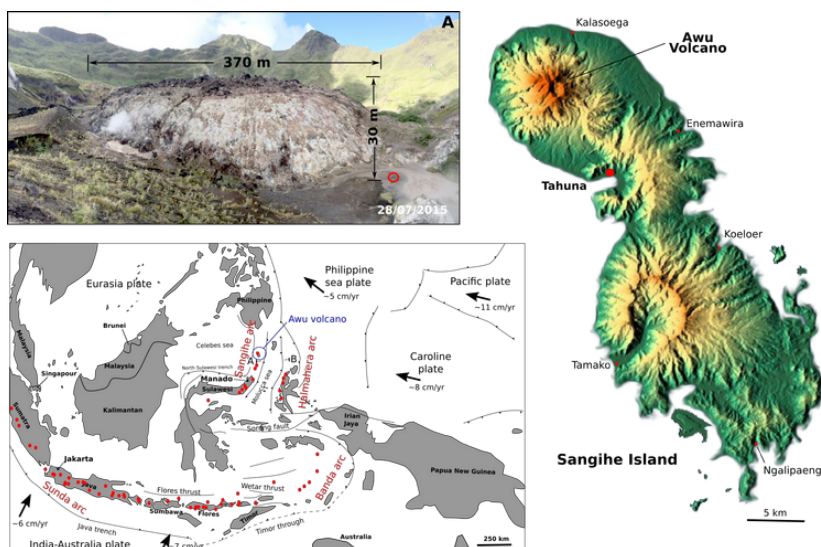


Figure 1. Awu volcano is the northernmost active volcano of the Sangihe arc. It occupies the northern portion of Sangihe island (3D map from <https://maps-for-free.com>). A lave dome occupies the center of the crater. Note the person circled in red for scale.



Figure 2. Awa lava dome in the crater. Degassing occurs from the lower crater wall and the northern part of the crater is the main degassing zone. The positions of DOAS scanning, MultiGAS (MG) and Infrared Camera are highlighted. The arrow of the IR_cam denotes the direction of the thermal camera.

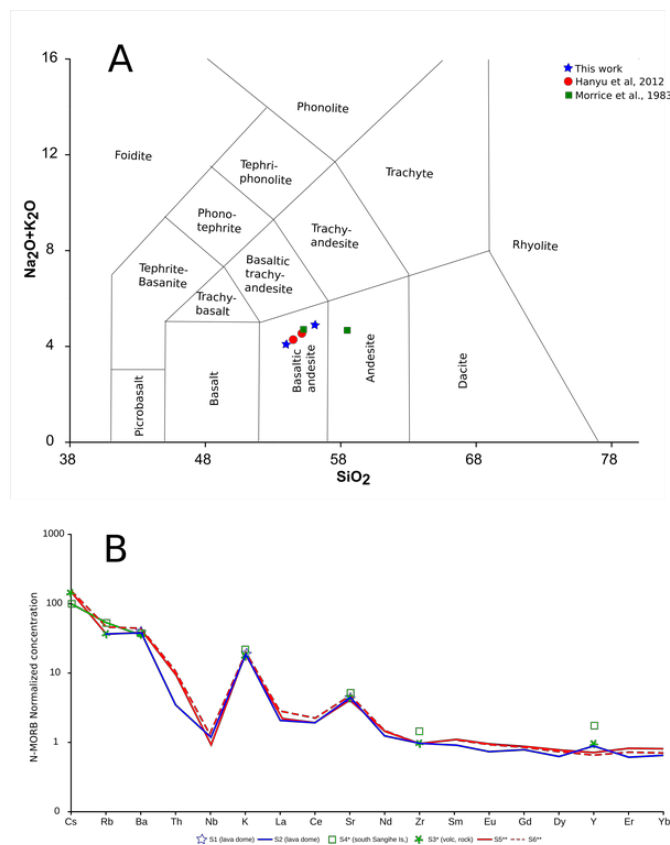


Figure 3. (A) Awu melt source is of basaltic andesite composition. Note that the sample from the southern part of Sangihe island (Morrice et al., 1983) rather indicates an andesite source. (B) Trace elements normalized to N-MORB indicate elevated ratios of LILE, LREE HFSE.

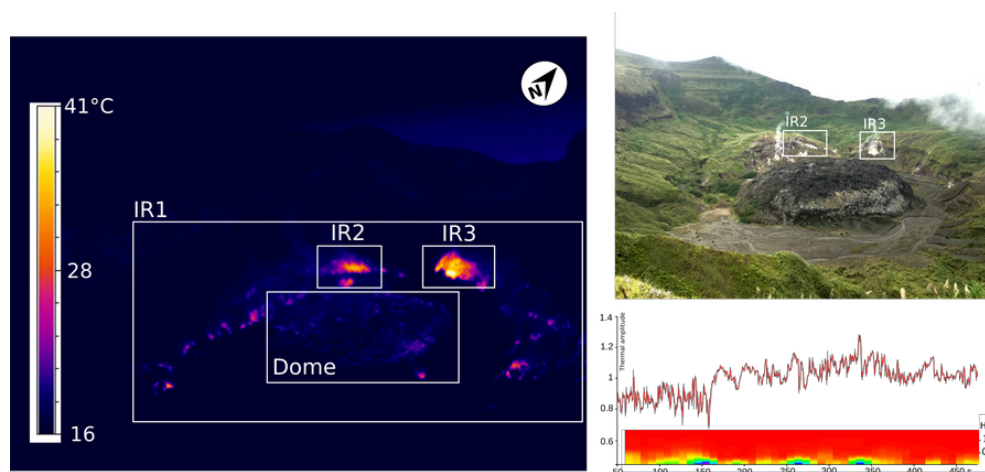


Figure 4. Thermal image highlighting the two most heated surfaces in the crater, as well as the lava dome being less hotter than the surrounding surface. White rectangles (IR1, IR2, IR3 and Dome) are the zones of interest in the radiant flux calculation (Table 3). The picture on the right gives a global view of the dome and its surroundings. The continuous thermal recording highlights a degassing dynamic through the IR3 zone characterized by a thermal fluctuation amplitude of 0.1-0.3 MW and at 0.3-0.4 Hz.

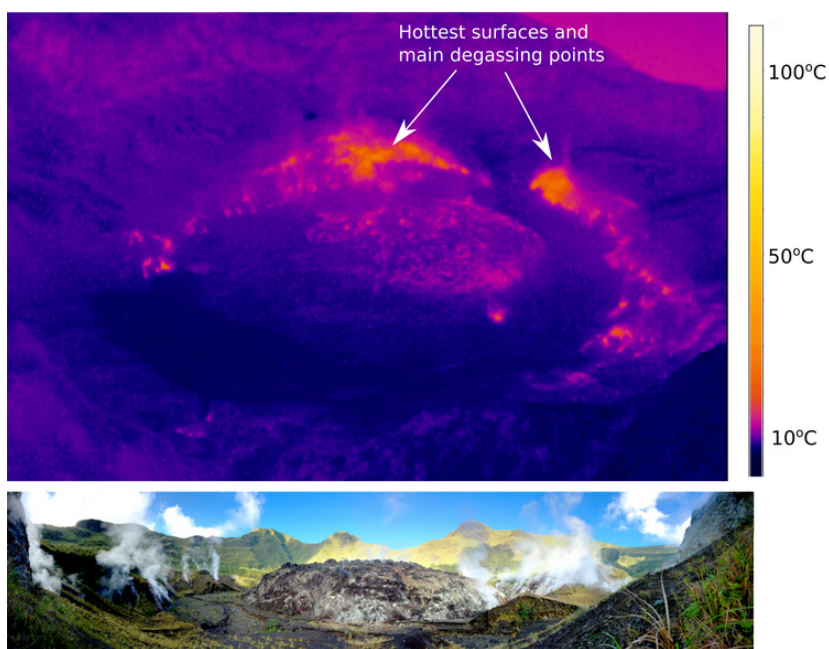


Figure 5. The lava dome and the conduit plug force the degassing to the crater wall. The hot surfaces (photo above) also correspond to the degassing points (picture below).

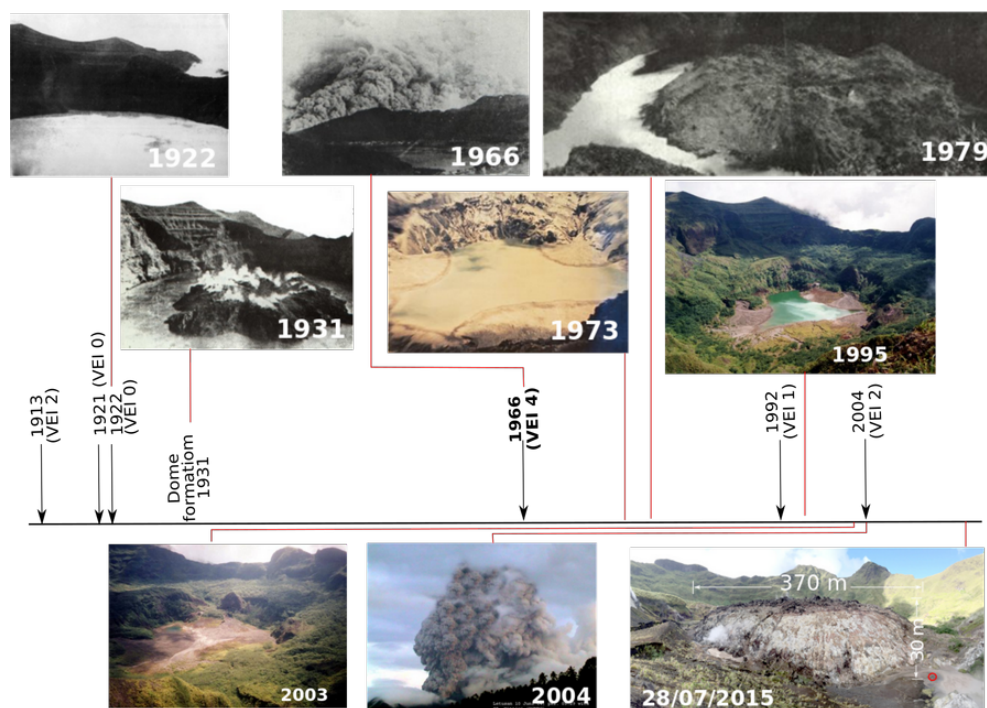


Figure 6. The configuration in Awu's crater is subjected to evolve from crater lake to lava dome emplacement and also from unoccupied crater to coexistence of lava dome and crater lake. Pictures from GVP, 2013 (Awu) except the 2015 (this work).

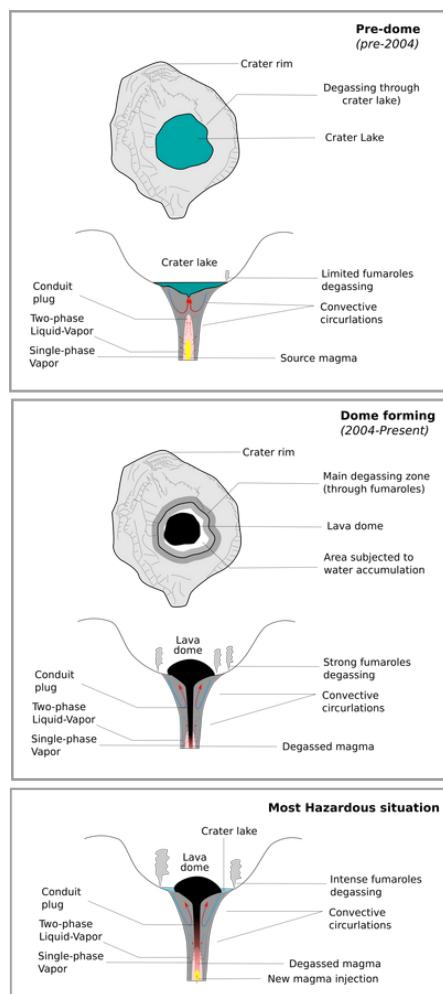


Figure 7. Pre-dome situation: A crater lake in Awu's crater. Few fumaroles on the crater wall. Dome forming situation: Lava dome emerged at the surface leading to lake water dry-out. Numerous fumaroles around the lava dome due to conduit plug. Most Hazardous situation: The cooled lava dome allowed the formation of a new crater lake. The new magma injection may enhance the opening of the conduit plug, leading to subsequent explosive water-magma interaction.